ACS OMEGA

http://pubs.acs.org/journal/acsodf

Article

Multilevel Simultaneous Lighting−Imaging System

Kang Fu,[§] Jianwei Fu,[§] Feifei Qin, Xumin Gao, Ziqi Ye, Pengzhan Liu, and Yongjin Wang*

Cite This: *ACS Omega* 2023, 8, 19987−19993

Read Online

ACCESS | Metrics & More | Article Recommendations | Supporting Information

ABSTRACT: In a III-nitride multiple quantum well (MQW) diode biased with a forward voltage, electrons recombine with holes inside the MQW region to emit light; meanwhile, the MQW diode utilizes the photoelectric effect to sense light when higher-energy photons hit the device to displace electrons in the diode. Both the injected electrons and the liberated electrons are gathered inside the diode, thereby giving rise to a simultaneous emission-detection phenomenon. The 4 × 4 MQW diodes could translate optical signals into electrical ones for image construction in the wavelength range from 320 to 440 nm. This technology will change the role of MQW diode-based displays since it can simultaneously transmit and receive optical signals, which is of crucial importance to the accelerating trend of multifunctional, intelligent displays using MQW diode technology.

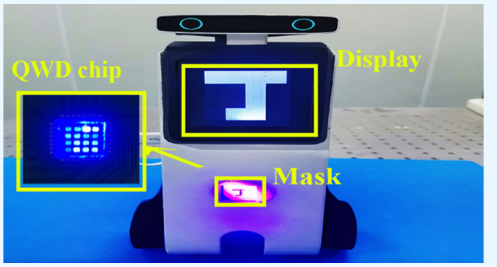

INTRODUCTION

The development of communication technology and materials science has heralded the era of the Internet of Things, which has also led to a level of diversity in modern display technology. Choi et al.[1] reported a fully operational 46-in. smart textile lighting/display system, Han et al.[2] demonstrated a simulation for a diffractive liquid crystal smart window for privacy applications, and Wakunami et al.[3] showed a projection-type holographic three-dimensional display in which a digitally designed holographic optical element and a digital holographic projection technique were combined. Meng et al.[4] demonstrated the integration of large-area MoS_2 thin-film transistors (TFTs) with nitride light-emitting diodes (LEDs) and demonstrated high-resolution displays. Jeong et al.[5] demonstrated textile-based organic electroluminescence displays (OLEDs). In addition, photoelectric display and detection methods have been developed and applied in increasing numbers. Gong et al.[6] discussed the future research directions of laser techniques in Micro-LED displays. Mikulics et al.[7] reported a device that can decrease energy consumption and increase computational operation speed. Hu et al.[8] analyzed a high-performance conical nanostructured GaN-based photodetector. Mikulics et al.[9] also researched the Nano-LED-driven phase change evolution of layered chalcogenides. Zhu et al.[10] discussed and summarized the recent two-dimensional materials. These studies involve biology, materials science, electronics, chemistry, and other disciplines, and an increasing number of studies are leading the development of modern display technology to a new stage.[11−14] However, there is seldom a way to give consideration to the advantages of both cost and versatility, which is a pain point and a blind spot for the current development of smart displays.[15,16] The development of the next generation of intelligent displays urgently requires dual-function devices.[17,18] Oh et al.[19] reported a double heterojunction nanorod device that can be used for simultaneous light emission and detection. Using a bifunctional perovskite diode, Shan et al.[20] proposed a bidirectional optical link between two identical devices. Some studies have shown that MQW diodes can not only be used for lighting and displays in the traditional sense but can also be used for the modulation and perception of light, which is termed the simultaneous emission-detection phenomenon.[21−25] Based on this phenomenon, we have confirmed that the communication performance of such diodes meets the requirements of duplex video transmission,[26] and after large-scale integration, optical signals containing on−off information can be scanned and detected.[27] With the advent of the era of high-speed communication, optical communication technology, a supplementary means of communication, has also made great progress.[28−35] The information exchange in this work is based on light, so it is suitable for the experimental scheme of traditional optical communication. In terms of hardware, we can carry out dual-function simultaneous driving of the emission and detection mode.[36−39] In terms of software, we can explore the signal restoration algorithm.[40−42] However, these findings fall short of the next generation of smart screens because the binarization of detection values leads to a quantization order for imaging grayscale that is too small, which is a problem that we have not discussed previously.

Shorter-wavelength light photons hit the MQW diode to create a photocurrent, which depends on the power of the

Received: March 28, 2023
Accepted: May 12, 2023
Published: May 22, 2023

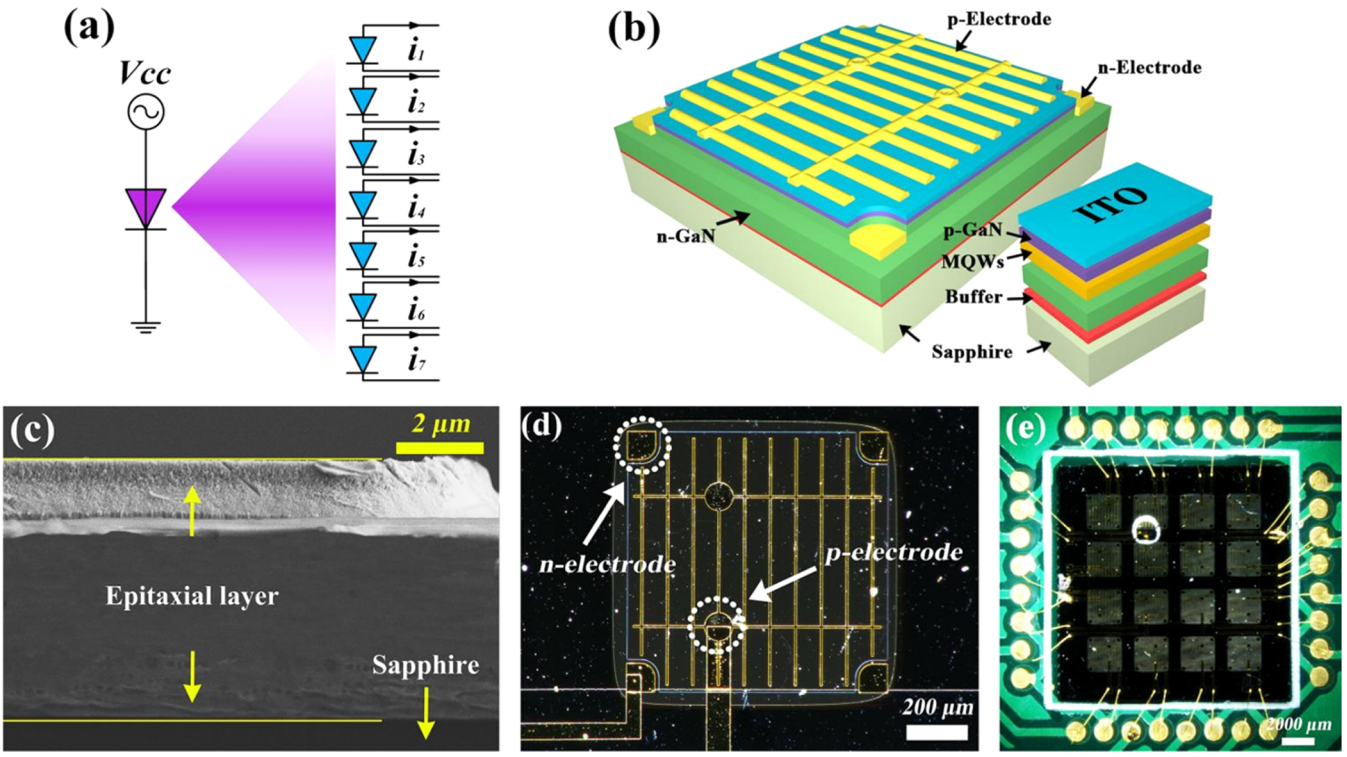

Figure 1. (a) Four hundred and five nanometer violet light was used as an external light source to stimulate a row of blue MQW diodes, and the difference in photocurrent generated by chips at different positions is compared. (b) A hierarchical structure diagram of the MQW diode. (c) SEM view of the MQW diode. (d) Optical microscope image of a single MQW diode. (e) Optical microscope image of the MQW diode arrays.

incident light. In fact, in this study, we quantized the value detected by the MQW diode with multiresolution to achieve multiscale character restoration and verified the experiment from both optical and electrical aspects. In addition, we tested the bandwidth of the array chip via 16-QAM modulation simulation[43] and confirmed that it retains a multimetric detection capability during high-speed optical communication. Finally, a prototype of the next-generation smart screen was formed, and its imaging ability was tested at the pixel level through an optical mold combined with the optical system, confirming that it shows potential for simultaneous display-imaging operation in practical scenarios. This work is enlightening for the realization of the next generation of smart screens and provides a new means for security monitoring, which is of great significance for the development of wireless optical communications in the future.[44,45]

DESIGN AND FABRICATION

The MQW diode was excited by light, thus generating a reverse photocurrent. We quantized and encoded this photocurrent to the signal processing unit for processing. As shown in Figure 1a, we used 405 nm violet light as the external light source to stimulate a row of blue MQW diodes. The blue MQW diode at the center of the violet spot clearly reached the maximum optical power. Experimental measurements showed that $i_4 > i_3 \approx i_5 > i_2 \approx i_6 > i_1 \approx i_7$, demonstrating that the position and intensity of external light can be encoded at multiple scales.

The selected MQW diode was characterized based on its morphology and data. Figure 1b shows a hierarchical structure diagram of the selected MQW diode in this paper, in which the p-electrode is connected to the positive electrode of the circuit, and the n-electrode is connected to the ground point of the circuit. Figure 1c shows a scanning electron microscope (SEM) view of the MQW diode. The sapphire substrate of the device is about 200 μm, while in the epitaxial layer, the n-GaN is about 5 μm and the rest is about 1.5 μm, and the total of the device is about 6.5 μm. Figure 1d shows an optical microscope image of a single MQW diode. Around the diode are n-GaN metal electrodes, forming a square-like shape with sides of about 100 μm. The metal electrodes of p-GaN/ITO are distributed over the entire surface of the device, forming an area of about 980 μm × 940 μm. The marks are the parts in contact with the external signal. Figure 1e shows an optical microscope picture of the MQW diode arrays, with a scale of 4 × 4 pixels and an overall shape of 11.68 mm square. As shown in the figure, gold wires were drawn from the p- and n-electrodes of the chip and connected to the pads on the printed circuit board (PCB) to form a common cathode structure. This array chip was used as the core chip to build the multiresolution smart screen system studied in this paper.

Before building the system, we need to discuss its feasibility. First, the external 405 nm light source was tested, and its optical power was recorded at different positions and different driving currents. To explain the data more comprehensively, we tested the optical power under different conditions, as shown in Table 1.

Table 1. Values on PM100D When λ = 405 nm

current distance	60 mm	40 mm	20 mm	0 mm
0 mA	0 mW	0 mW	0 mW	0 mW
20 mA	2.4 mW	13.6 mW	20.1 mW	31.4 mW
40 mA	18.4 mW	25.5 mW	39.8 mW	45.5 mW
60 mA	38.3 mW	49.0 mW	52.0 mW	56.2 mW

https://doi.org/10.1021/acsomega.3c02072
ACS Omega 2023, 8, 19987−19993

We characterized the coexistence of emission and detection for MQW diodes from the perspective of electricity. Therefore, we used a Keithley 2636b digital original table to scan the $I-V$ characteristics of the chip, and the scanning curve is shown by the blue line in Figure 2. With increasing voltage from − 2 to

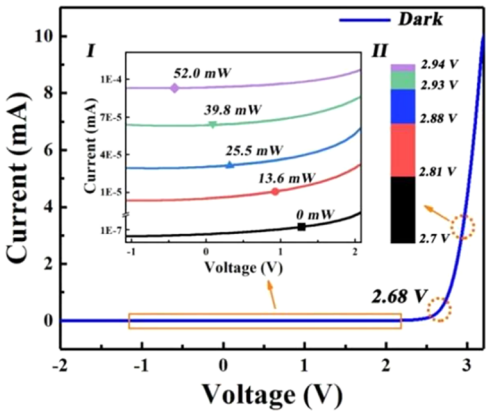

Figure 2. $I-V$ curve measured under the irradiation of external violet light sources with different optical powers.

3.2 V, the MQW diode turned on near 2.68 V, and the current sharply increased. For a voltage of less than 2.68 V, the data shown in Table 1 were used for reference to irradiate the MQW diode to be tested with violet light sources of different powers. Figure 2(I) shows the $I-V$ curve measured under the irradiation of external violet light sources with different optical powers. When the optical power was 0 mW, that is, in the absence of external interference, the dark current was $\sim 1 \times 10^{-7}$ mA. At an optical power of 13.6 mW, the current was a superposition of the dark current and photocurrent, with a magnitude of $\sim 10^{-5}$ mA. As the power of the external light source gradually increased, the current also gradually increased. For an external violet light source power of 52 mW, the circuit current reached 10^{-4} mA. This finding confirms that the detection effect was achieved when the MQW diode was turned off and could be quantified according to the optical power. At the on voltage for the chip, we used the light source with the same power to irradiate the MQW diode to be measured, and the results are shown in Figure 2. Because the change in photocurrent was very small compared with the driving current, we added a resistance of 1 kΩ to convert the current signal into a voltage signal for clear observation. When the external violet light source was not turned on (0 mW), the voltage of the blue light diode chip to be tested remained unchanged at 2.7 V. When the power of the external violet light source was gradually increased to 13.6, 25.5, 39.8, and 52.0 mW, the voltage gradually increased to 2.81, 2.88, 2.93, and 2.94 V. This finding confirms the coexistence of emission and detection. Furthermore, the excited photocurrent also increased with increasing external excitation, and the added value could be quantized after signal processing. This finding confirms that MQW diode arrays can be used to realize a multifunctional smart screen for simultaneous light detection and display.

To explore the essence of the coexistence phenomenon for emission and detection using MQW diodes, we used a semiconductor device analyzer B1500A to characterize the optical characteristics of the diode. The electroluminescence (EL) spectra for the blue MQW diode to be measured and the external purple light source are plotted as a function of the injection current in Figure 3a. For a distance of 60 mm and a driving current of 20 mA, the luminous intensity was slightly stronger than that of the chip to be tested due to the focusing of the external light source, and the dominant spectral peak was observed at a wavelength of 404.45 nm. The blue light MQW diode to be tested could be used as the emitter. When the external driving voltage was less than 2.68, 2.7, 2.8, and 2.9 V, respectively, the chip converted electric energy and information into optical information for transmission. This behavior corresponds to a never-on-on process for the chip, and its luminous intensity gradually increases. The dominant peak occurred at a wavelength of 451.57 nm. Conversely, MQW diodes absorb photons and release electron−hole pairs to transcribe photons into electrons. We tested the detection spectrum for the MQW diode, set the bias voltage to − 2, 0, 2, 2.6, and 2.7 V, respectively, and observed the response curve for the chip. The results are shown in Figure 3b. The response of the diode was clearly observed to gradually decrease with increasing bias voltage. At a driving voltage of 2.7 V for the MQW diode, the device was in the on state, and its detection spectrum overlapped with the emission spectrum of the external violet light source by ∼10 nm, which confirms that the simultaneous emission and detection scheme was possible from an optical point of view. In order to test the efficiency of the diode device, we tested its external quantum efficiency (EQE) of detection at different voltages. The results are shown in Figure 3c. When the diode is off, the maximum efficiency is obtained near 328 nm, and when the voltage is near the

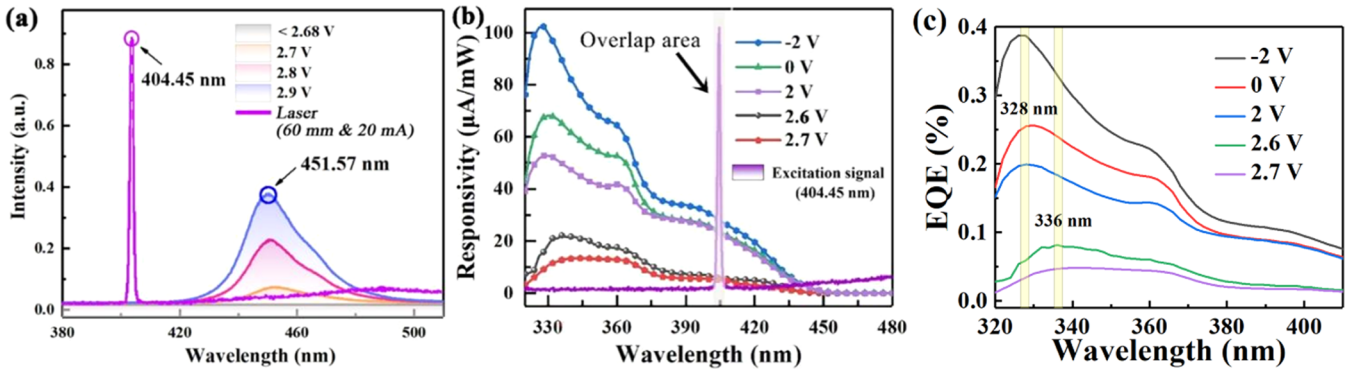

Figure 3. (a) Electroluminescence spectrum curve of the MQW diode under different bias voltages and the spectrum curve of external excitation light. (b) Optical explanation of the MQW diode with the capability of simultaneous emission and detection. (c) EQE of the MQW diode.

https://doi.org/10.1021/acsomega.3c02072
ACS Omega 2023, 8, 19987−19993

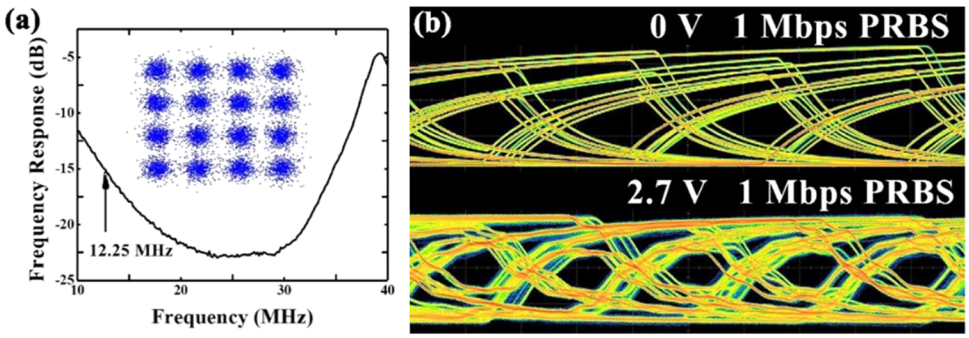

Figure 4. (a) Frequency response of the MQW chip. (b) Turn the MQW diode on and off, send a 1 Mbps PRBS signal, and observe its receiving eye diagram.

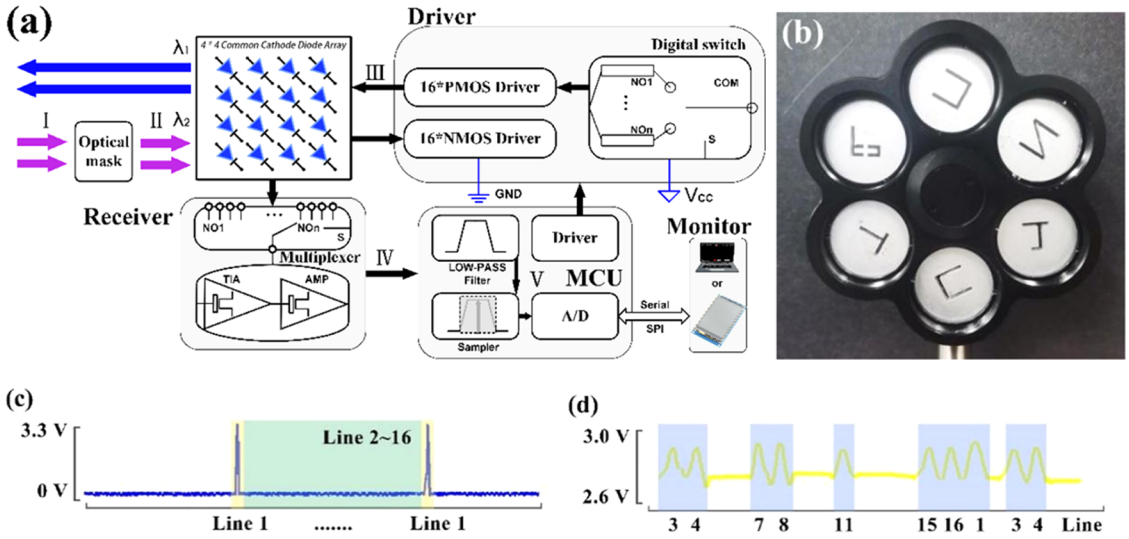

Figure 5. (a) Circuit block diagram of the system. (b) Optical molds used in this work. (c) Drive signal of the MQW diode arrays. (d) Signal analysis of different pixel units in the MQW diode arrays when receiving external light source stimulation.

opening voltage, the maximum efficiency is obtained near 336 nm; the efficiency decreases as the voltage increases.

Therefore, imaging can be accomplished with different gray levels based on MQW diode arrays. To explore the limit value for the chip and determine the speed range for smart screen scanning, we also tested the communication performance of the chip. We tested its frequency response with an ENA network analyzer E5080A, as shown in Figure 4a. The 3 dB bandwidth of this MQW diode is 12.25 MHz, so it meets the refresh speed required for most screen resolutions. We used MATLAB to perform 16-QAM modulation for the light source and used the MQW diode to receive the signal and then send it to the demodulation module. The constellation is shown in Figure 4a. A large Euclidean distance is clearly observed between different symbols, which indicates easy demodulation and good communication performance. When applied to the system, we used a signal generator to generate a 1 Mbps pseudorandom binary sequence (PRBS) waveform, which was loaded onto the violet light source for transmission. At the receiving end, the MQW diode under different bias voltages was used as the receiver to test the communication eye diagram for the signal. Consequently, when the MQW diode was turned off, that is, when no voltage was applied, eyes were clearly observed in the diagram, as shown in Figure 4b. Therefore, the decision threshold was easily determined. When the MQW diode was just turned on, that is, at a bias voltage of 2.7 V, the eyes in the eye diagram became distorted. This behavior is attributed to the interference of the direct current (DC) signal, which constitutes a large part of the photocurrent signal generated by the stimulation of the embedded chip. The signal could still be demodulated and quantized by using a suitable processing circuit.

RESULTS AND DISCUSSION

Therefore, we built the circuit and system shown in Figure 5a to generate a primary prototype for the next generation of smart screens. The 4 × 4 MQW diode arrays shown in the figure are the core part. It can be used as a transmitter to send out blue light at a wavelength of ∼450 nm, which intuitively shows the lighting display mode for the array. It can also be used as a receiver to receive external violet light at a wavelength of ∼405 nm. Transmission and reception can be performed simultaneously. For the external violet light source, the optical signal at position I can exist without image or character information. After passing through the optical mold, the light source was encoded to generate the optical signal with character information at position II. This optical mold is shown in Figure 5b, which can be customized according to user needs. For the transmission path, the upper computer informs the microprocessor of the content to be displayed, and the microprocessor controls the driving circuit through the input/output port. Specifically, the microprocessor controls the

https://doi.org/10.1021/acsomega.3c02072
ACS Omega 2023, 8, 19987−19993

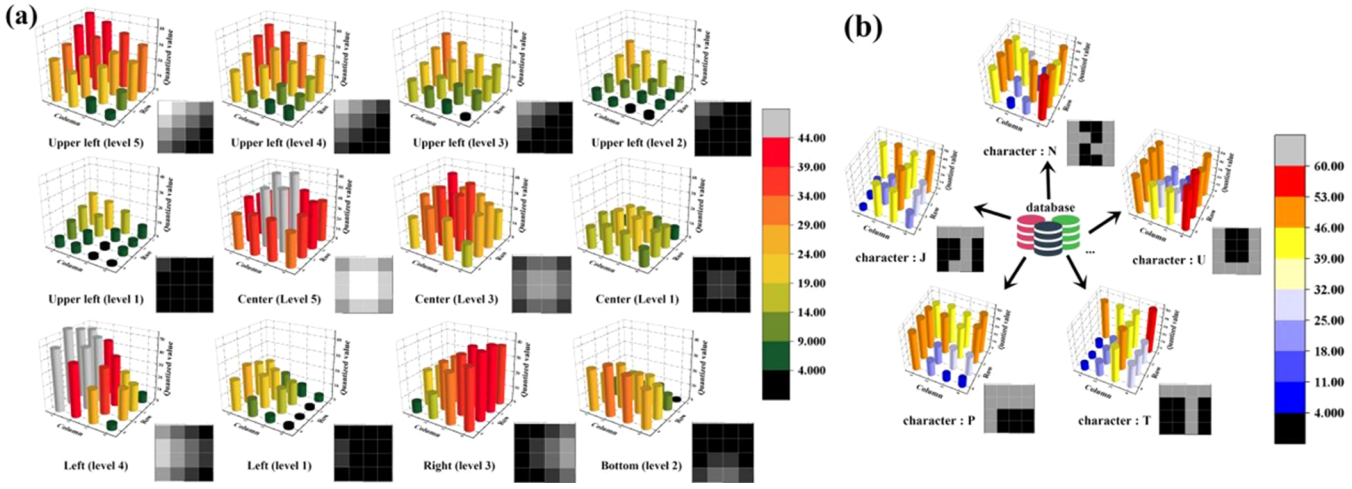

Figure 6. (a) Change the intensity of the excitation light, stimulate different positions of the MQW diode arrays, and record the experimental results. (b) Test of the MQW diode arrays for character imaging.

positive channel metal oxide semiconductor (PMOS) of the positive electrode and the negative channel metal oxide semiconductor (NMOS) of the negative electrode of the array chip through a multiplexer to scan the array chip and display the corresponding patterns. Figure 5c shows the array chip drive signal at III. Since 16 channels were used in this study in scanning mode, the drive signal arrived every 16 time slots and turned on the MOS transistor once. For the receiving path, the array chip converted the violet light signal carrying the character information into a photocurrent signal after receiving it. Then, a signal that could be received and recognized by the microprocessor was generated through a multiplexer, a transimpedance amplifier, and a diode amplifier. Figure 5d shows this signal, corresponding to IV in Figure 5a. At this time, the 1st, 3rd, 4th, 7th, 8th, 11th, 15th, and 16th diodes were excited to generate received signals with different amplitudes. Then, the microprocessor performed filtering, sampling, quantization, and corresponding coding according to the user's requirements for resolution. V in Figure 5a corresponds to this process. After encoding, the signal was sent to the upper computer or TFT screen module to display the imaging results. This process is the workflow for the entire system. Based on the above design, the core work for the next generation of smart screens is complete.

Part 1 in Visualization 1 shows the system composition. We conducted two tests on the system to verify its feasibility as a next-generation smart display screen.

Test 1: We used different optical powers to stimulate the array chip, observe its quantized value, and display an image on the user interface according to this value. The test results are shown in Figure 6a, and part 2 in Visualization 1 shows a recording of the specific test process. The value under dark field conditions was recorded here as the reference value for each reading. We can subtract the value excited by the external light source from this reference value as the basis for final quantification. If this value is divided into five gray levels based on the quantization values 25/30/35/40 (source: 5 V, quantization: 210), the array chip can be used to distinguish between excitation sources at different positions and different powers and perform correct imaging.

Test 2: We selected the optical mold with symbol information to encode the excitation source signal and then stimulated the array chip with the excitation source to observe the imaging results. The test results are shown in Figure 6b, and part 3 in Visualization 1 shows a recording of the specific test process. The array chip can also be used to correctly image the initial characters.

CONCLUSIONS

We confirmed that MQW diode arrays can be used as a core device for the next generation of smart screens, and they can be used as a display and a camera at the same time. Nevertheless, the implementation remains subject to some shortcomings; specifically, the scheme lacks the imaging of the three primary RGB colors. However, we can design MQW diodes with red, green, and blue primary colors by exploiting the coexistence of emission and detection. Bragg mirrors of corresponding wavelengths can be plated onto the chips to achieve optical filtering of the corresponding wavelengths. Finally, we can use the system to detect signals and form color images. In short, we propose a prototype for the next generation of smart screens that is based on MQW diode emission and detecting coexisting physical phenomena and has advantages in terms of multiresolution, scalability, and cost. In the era of the Internet of Things, this system provides great inspiration and has practical value, especially for intelligent display and confidential monitoring.

ASSOCIATED CONTENT

Data Availability Statement

The authors confirm that the data supporting the findings of this study are available within the article.

Supporting Information

The Supporting Information is available free of charge at https://pubs.acs.org/doi/10.1021/acsomega.3c02072.

A movie used for this imaging system is provided (Visualization 1) (MP4)

AUTHOR INFORMATION

Corresponding Author

Yongjin Wang − *GaN Optoelectronic Integration International Cooperation Joint Laboratory of Jiangsu Province, Nanjing University of Posts and Telecommunications, Nanjing 210003, China;* orcid.org/0000-0001-8109-4640; Email: wangyj@njupt.edu.cn

https://doi.org/10.1021/acsomega.3c02072
ACS Omega 2023, 8, 19987−19993

Authors

Kang Fu − *Grünberg Research Centre, Nanjing University of Posts and Telecommunications, Nanjing 210003, China;* orcid.org/0000-0003-1239-7685

Jianwei Fu − *Grünberg Research Centre, Nanjing University of Posts and Telecommunications, Nanjing 210003, China*

Feifei Qin − *Grünberg Research Centre, Nanjing University of Posts and Telecommunications, Nanjing 210003, China*

Xumin Gao − *Grünberg Research Centre, Nanjing University of Posts and Telecommunications, Nanjing 210003, China*

Ziqi Ye − *Grünberg Research Centre, Nanjing University of Posts and Telecommunications, Nanjing 210003, China*

Pengzhan Liu − *Grünberg Research Centre, Nanjing University of Posts and Telecommunications, Nanjing 210003, China*

Complete contact information is available at: https://pubs.acs.org/10.1021/acsomega.3c02072

Author Contributions

[§]K.F. and J.F. contributed equally to the article. K.F. conceived and designed the experiments, performed the experiments, analyzed the data, and wrote the paper. Y.W. designed and fabricated the chips and proposed and coordinated the overall project. X.G., J.F., and P.L. performed the experiments. F.Q. analyzed the data. All authors reviewed the manuscript.

Notes

The authors declare no competing financial interest.

■ ACKNOWLEDGMENTS

This work was jointly supported by the National Key Research and Development Program of China (2022YFE0112000), 111 Project (D17018), and National Natural Science Foundation of China (61827804 and U21A201550), Jiangsu Province Innovation Plan Project (KYCX22_0935).

■ REFERENCES

(1) Choi, H. W.; Shin, D. W.; Yang, J.; Lee, S.; Figueiredo, C.; Sinopoli, S.; Ullrich, K.; Jovančić, P.; Marrani, A.; Momentè, R.; et al. Smart textile lighting/display system with multifunctional fibre devices for large scale smart home and IoT applications. *Nat. Commun.* **2022**, *13*, No. 814.

(2) Han, C. H.; Eo, H.; Choi, T. H.; Kim, W. S.; Oh, S. W. A simulation of diffractive liquid crystal smart window for privacy application. *Sci. Rep.* **2022**, *12*, No. 11384.

(3) Wakunami, K.; Hsieh, P. Y.; Oi, R.; Senoh, T.; Sasaki, H.; Ichihashi, Y.; Okui, M.; Huang, Y. P.; Yamamoto, K. Projection-type see-through holographic three-dimensional display. *Nat. Commun.* **2016**, *7*, No. 12954.

(4) Meng, W.; Xu, F.; Yu, Z.; Tao, T.; Shao, L.; Liu, L.; Li, T.; Wen, K.; Wang, J.; He, L.; et al. Three-dimensional monolithic micro-LED display driven by atomically thin transistor matrix. *Nat. Nanotechnol.* **2021**, *16*, 1231.

(5) Jeong, S. Y.; Shim, H. R.; Na, Y.; Kang, K. S.; Jeon, Y.; Choi, S.; Jeong, E. G.; Park, Y. C.; Cho, H.-E.; Lee, J.; et al. Foldable and washable textile-based OLEDs with a multi-functional near-room-temperature encapsulation layer for smart e-textiles. *npj Flex. Electron.* **2021**, *5*, No. 15.

(6) Gong, Y.; Gong, Z. Laser-Based Micro/Nano-Processing Techniques for Microscale LEDs and Full-Color Displays. *Adv. Mater. Technol.* **2023**, *8*, No. 2200949.

(7) Mikulics, M.; Hardtdegen, H. H. Fully photon operated transmistor/all-optical switch based on a layered $Ge_1Sb_2Te_4$ phase change medium. *FlatChem* **2020**, *23*, No. 100186.

(8) Hu, T.; Li, X.; Liu, C.; Lin, S.; Wang, K.; Liu, J.; Zhao, L. High performance conical nanostructured GaN-based photodetectors. *J. Phys. D: Appl. Phys.* **2022**, *55*, No. 035102.

(9) Mikulics, M.; Adam, R.; Sobolewski, R.; Heidtfeld, S.; Cao, D.; Bürgler, D. E.; Schneider, C. M.; Mayer, J.; Hardtdegen, H. H. Nano-LED driven phase change evolution of layered chalcogenides for Raman spectroscopy investigations. *FlatChem* **2022**, *36*, No. 100447.

(10) Zhu, M.; Huang, K.; Zhou, K.-G. Lifting the mist of flatland: The recent progress in the characterizations of two-dimensional materials. *Prog. Cryst. Growth Charact. Mater.* **2017**, *63*, 72−93.

(11) Wen, G.-Y.; Zhou, X.-L.; Tian, X.-Y.; Xie, R.; Ju, X.-J.; Liu, Z.; Faraj, Y.; Wang, W.; Chu, L.-Y. Smart hydrogels with wide visible color tunability. *NPG Asia Mater.* **2022**, *14*, 29.

(12) He, X.; Cui, Y.; Tentzeris, M. M. Tile-based massively scalable MIMO and phased arrays for 5G/B5G-enabled smart skins and reconfigurable intelligent surfaces. *Sci. Rep.* **2022**, *12*, No. 2741.

(13) Jemmali, M.; Melhim, L. K. B.; Alharbi, M. T.; Bajahzar, A.; Omri, M. N. Smart-parking management algorithms in smart city. *Sci. Rep.* **2022**, *12*, No. 6533.

(14) Xie, C.; Zhao, X.; Ong, E. W. Y.; Tan, Z.-K. Smart-parking management algorithms in smart city. *Nat. Commun.* **2020**, *11*, No. 4213.

(15) Sekitani, T.; Nakajima, H.; Maeda, H.; Fukushima, T.; Aida, T.; Hata, K.; Someya, T. Stretchable active-matrix organic light-emitting diode display using printable elastic conductors. *Nat. Mater.* **2009**, *8*, 494.

(16) Sabbar, A.; Madhusoodhanan, S.; Al-Kabi, S.; Dong, B.; Wang, J.; Atcitty, S.; Kaplar, R.; Ding, D.; Mantooth, A.; Yu, S.-Q.; Chen, Z. High temperature and power dependent photoluminescence analysis on commercial lighting and display LED materials for future power electronic modules. *Sci. Rep.* **2019**, *9*, No. 16758.

(17) Gao, X.; Liu, P.; Yin, Q.; Wang, H.; Fu, J.; Hu, F.; Jiang, Y.; Zhu, H.; Wang, Y. Wireless light energy harvesting and communication in a waterproof GaN optoelectronic system. *Commun. Eng.* **2022**, *1*, 16.

(18) Gong, C.-S. A.; Lee, Y.-C.; Lai, J.-L.; Yu, C.-H.; Huang, L. R.; Yang, C.-Y. The high-efficiency LED driver for visible light communication applications. *Sci. Rep.* **2016**, *6*, No. 30991.

(19) Oh, N.; Kim, B. H.; Cho, S. Y.; Nam, S.; Rogers, S. P.; Jiang, Y.; Flanagan, J. C.; Zhai, Y.; Kim, J. H.; Lee, J.; et al. Double-heterojunction nanorod light-responsive LEDs for display applications. *Science* **2017**, *355*, 616.

(20) Shan, Q.; Wei, C.; Jiang, Y.; Song, J.; Zou, Y.; Xu, L.; Fang, T.; Wang, T.; Dong, Y.; Liu, J.; et al. Perovskite light-emitting/detecting bifunctional fibres for wearable LiFi communication. *Light: Sci. Appl.* **2020**, *9*, 163.

(21) Wang, Y.; Wang, X.; Zhu, B.; Shi, Z.; Yuan, J.; Gao, X.; Liu, Y.; Sun, X.; Li, D.; Amano, H. Full-duplex light communication with a monolithic multicomponent system. *Light: Sci. Appl.* **2018**, *7*, 83.

(22) Wang, Y.; Zhu, G.; Cai, W.; Gao, X.; Yang, Y.; Yuan, J.; Shi, Z.; Zhu, H. On-chip photonic system using suspended p-n junction InGaN/GaN multiple quantum wells device and multiple waveguides. *Appl. Phys. Lett.* **2016**, *108*, No. 162102.

(23) Wang, Y.; Wang, S.; Ni, S.; Wang, W.; Shi, Z.; Yuan, J.; Zhu, H. On-chip multicomponent system made with vertical structure QWD. *Semicond. Sci. Technol.* **2019**, *34*, No. 065017.

(24) Wang, Y.; Xu, Y.; Yang, Y.; Gao, X.; Zhu, B.; Cai, W.; Yuan, J.; Zhang, R.; Zhu, H. Simultaneous light emission and detection of InGaN/GaN multiple QWDs for in-plane visible light communication. *Opt. Commun.* **2017**, *387*, 440.

(25) Gao, X.; Shi, Z.; Zhu, B.; Wu, F.; Yuan, J.; Qin, C.; Jiang, Y.; Cai, W.; Wang, Y. Tandem dual-functioning multiple-quantum-well diodes for a self-powered light source. *Opt. Lett.* **2018**, *43*, 3710.

(26) Fu, K.; Gao, X.; Ye, Z.; Li, J.; Ji, X.; Wang, Y. Coexistence of light emission and detection in a III-nitride QWD. *Opt. Lett.* **2022**, *47*, 2614.

(27) Fu, K.; et al. Simultaneous ilemission-imaging. *Adv. Mater. Technol.* **2021**, *6*, No. 2100227.

(28) Shi, Z.; Yuan, J.; Zhang, S.; Liu, Y.; Wang, Y. Simultaneous dual-functioning InGaN/GaN multiple-quantum-well diode for transferrable optoelectronics. *Opt. Mater.* **2017**, *72*, 20.
(29) Li, X.; Wang, Y.; Hane, K.; Shi, Z.; Yan, J. GaN-based integrated photonics chip with suspended LED and waveguide. *Opt. Commun.* **2018**, *415*, 43.
(30) Nargelas, S.; Mickevičius, J.; Kadys, A.; Jarašiūnas, K.; Malinauskas, T. Stimulated emission threshold in thick GaN epilayers: interplay between charge carrier and photon dynamics. *Opt. Laser Technol.* **2021**, *134*, No. 106624.
(31) Sarwar, A. G.; Carnevale, S. D.; Yang, F.; Kent, T. F.; Jamison, J. J.; McComb, D. W.; Myers, R. C. Semiconductor nanowire light-emitting diodes grown on metal: a direction toward large-scale fabrication of nanowire devices. *Small* **2015**, *11*, 5402.
(32) Feng, M.; Wang, J.; Zhou, R.; Sun, Q.; Gao, H.; Zhou, Y.; Liu, J.; Huang, Y.; Zhang, S.; Ikeda, M.; et al. On-chip integration of GaN-based laser, modulator, and photodetector grown on Si. *IEEE J. Sel. Top. Quantum Electron.* **2018**, *24*, No. 8200305.
(33) Peng, M.; Li, Z.; Liu, C.; Zheng, Q.; Shi, X.; Song, M.; Zhang, Y.; Du, S.; Zhai, J.; Wang, Z. L. High-resolution dynamic pressure sensor array based on piezo-phototronic effect tuned photoluminescence imaging. *ACS Nano* **2015**, *9*, 3143.
(34) Heo, S. Y.; Kim, J.; Gutruf, P.; Banks, A.; Wei, P.; Pielak, R.; Balooch, G.; Shi, Y.; Araki, H.; Rollo, D.; et al. Wireless, battery-free, flexible, miniaturized dosimeters monitor exposure to solar radiation and to light for phototherapy. *Sci. Transl. Med.* **2018**, *10*, No. eaau1643.
(35) Nikoobakht, B.; Hansen, R. P.; Zong, Y.; Agrawal, A.; Shur, M.; Tersoff, J. High-brightness lasing at submicrometer enabled by droop-free fin light-emitting diodes (LEDs). *Sci. Adv.* **2020**, *6*, No. eaba4346.
(36) Li, J.; Ye, D.; Fu, K.; Wang, L.; Piao, J.; Wang, Y. Single-photon detection for MIMO underwater wireless optical communication enabled by arrayed LEDs and SiPMs. *Opt. Express* **2021**, *29*, 25922.
(37) Ren, A.; Wang, H.; Zhang, W.; Wu, J.; Wang, Z.; Penty, R. V.; White, I. H. Emerging light-emitting diodes for next-generation data communications. *Nat. Electron.* **2021**, *4*, 559.
(38) Zhang, J.-F.; Yi, Q.-W.; Li, J. Complex analytic wavelet transform and vibration signals envelope-demodulation analysis. *J. Vib. Shock* **2010**, *29*, 93.
(39) Taylor, M. G. Coherent detection method using DSP for demodulation of signal and subsequent equalization of propagation impairments. *IEEE Photonics Technol. Lett.* **2004**, *16*, 674.
(40) Ates, S.; Agha, I.; Gulinatti, A.; Rech, I.; Badolato, A.; Srinivasan, K. Improving the performance of bright quantum dot single photon sources using temporal filtering via amplitude modulation. *Sci. Rep.* **2013**, *3*, No. 1397.
(41) Du, C.; Huang, X.; Jiang, C.; Pu, X.; Zhao, Z.; Jing, L.; Hu, W.; Wang, Z. L. Tuning carrier lifetime in InGaN/GaN LEDs via strain compensation for high-speed visible light communication. *Sci. Rep.* **2016**, *6*, No. 37132.
(42) Zhang, J.; Alam, P.; Zhang, S.; Shen, H.; Hu, L.; Sung, H. H. Y.; Williams, I. D.; Sun, J.; Lam, J. W. Y.; Zhang, H.; Tang, B. Z. Secondary through-space interactions facilitated single-molecule white-light emission from clusteroluminogens. *Nat. Commun.* **2022**, *13*, No. 3492.
(43) Maher, R.; Xu, T.; Galdino, L.; Sato, M.; Alvarado, A.; Shi, K.; Savory, S. J.; Thomsen, B. C.; Killey, R. I.; Bayvel, P. Spectrally shaped DP-16QAM super-channel transmission with multi-channel digital back-propagation. *Sci. Rep.* **2015**, *5*, No. 8214.
(44) Zhang, X. G.; Sun, Y. L.; Zhu, B.; Jiang, W. X.; Yu, Q.; Tian, H. W.; Qiu, C.-W.; Zhang, Z.; Cui, T. J. A metasurface-based light-to-microwave transmitter for hybrid wireless communications. *Light: Sci. Appl.* **2022**, *11*, 126.
(45) Karothu, D. P.; Dushaq, G.; Ahmed, E.; Catalano, L.; Polavaram, S.; Ferreira, R.; Li, L.; Mohamed, S.; Rasras, M.; Naumov, P. Mechanically robust amino acid crystals as fiber-optic transducers and wide bandpass filters for optical communication in the near-infrared. *Nat. Commun.* **2021**, *12*, No. 1326.

https://doi.org/10.1021/acsomega.3c02072
ACS Omega 2023, 8, 19987−19993